



**The interplay of fibronectin functionalization and TGF- $\beta$ 1 presence on fibroblast proliferation, differentiation and migration in 3D matrices**

Journal:	<i>Biomaterials Science</i>
Manuscript ID:	BM-ART-04-2015-000140.R1
Article Type:	Paper
Date Submitted by the Author:	03-Jun-2015
Complete List of Authors:	Sapudom, Jiranuwat; Institute of Biochemistry, Biophysical Chemistry Stefan, Rubner; Universität Leipzig, Institute of Biochemistry Martin, Steve; Leipzig University, Institute of Biochemistry Thoenes, Stephan; Universitätsklinikum Leipzig, Department of Dermatology, Venerology and Allergology Anderegg, Ulf; Universitätsklinikum Leipzig, Department of Dermatology, Venerology and Allergology Pompe, Tilo; Universität Leipzig, Institute of Biochemistry

## The interplay of fibronectin functionalization and TGF- $\beta$ 1 presence on fibroblast proliferation, differentiation and migration in 3D matrices

Jiranuwat Sapudom,<sup>a</sup> Stefan Rubner,<sup>a</sup> Steve Martin,<sup>a</sup> Stephan Thoenes,<sup>b</sup>  
Ulf Anderegg,<sup>b</sup> Tilo Pompe<sup>a,\*</sup>

<sup>a</sup> Institute of Biochemistry, Faculty of Biosciences, Pharmacy and Psychology, Universität Leipzig, Leipzig 04103, Germany.

<sup>b</sup> Department of Dermatology, Venereology and Allergology, Universitätsklinikum Leipzig, Leipzig 04103, Germany

\* To whom correspondence should be addressed

Tilo Pompe

Postal address:           Universität Leipzig  
                                  Institute of Biochemistry  
                                  Johannisallee 21-23  
                                  04103 Leipzig  
                                  Germany

Phone/Fax:               +49 341 97 36931/9

Email:                     [tilo.pompe@uni-leipzig.de](mailto:tilo.pompe@uni-leipzig.de)

**Abstract**

Defined biomimetic three-dimensional (3D) matrices are needed to decipher the complex cellular signalling during wound healing at high resolution *in vitro*. Soluble factors like TGF- $\beta$ 1 and adhesion promoting structural components of the extracellular matrix (ECM) are known to be key regulators of fibroblast behaviour. The ECM component fibronectin (FN) bears a complex function as adhesion promoter, fibrillar element and soluble factor binder. However, its implementation in biomimetic 3D matrices is frequently ill defined. To study the impact of FN on fibroblast cellular function under differentiating conditions (TGF- $\beta$ 1 stimulation), we functionalized 3D collagen I matrices with FN using two strategies: co-assembly and adsorptive immobilization. In comparison to co-assembly, adsorptive immobilization provided no alteration in collagen microstructure as well as mechanical properties. Moreover, this approach provided a controllable FN amount and a homogenous distribution of FN throughout collagen networks. A strong interplay of FN amount and TGF- $\beta$ 1 stimulation on fibroblast function was found in terms of proliferation, migration and myofibroblast differentiation. High levels of FN alone reduced proliferation and showed no effect on differentiation of fibroblasts, but increased migration. In contrast, fibroblast stimulation with high amounts of FN together with TGF- $\beta$ 1 increased proliferation. Independent of FN, the TGF- $\beta$ 1 stimulation enhanced mRNA expression of matrix components like collagen type I alpha 1 chain (Coll I(a1)), FN with extra domain A (EDA-FN) and reduced cell migration. The latter cell behaviour indicated a FN independent differentiation into a myofibroblast phenotype. Overall, our 3D biomimetic matrices allow dissecting the overlapping action of the ECM protein FN and the soluble factor TGF- $\beta$ 1 on fibroblast proliferation, migration and differentiation in 3D microenvironments. Furthermore, this model enables the mimicking of important steps of the *in vivo* wound healing process *in vitro*.

**Keywords:**

collagen I; fibronectin; 3D matrix; fibroblasts; myofibroblast; transforming factor beta 1(TGF- $\beta$ 1); wound healing

## 1 Introduction

Wound healing is a multi-step process resulting from complex signalling between cells and their microenvironment, the extracellular matrix (ECM). ECM is integral to each phase of wound healing by interacting with cells and soluble factors<sup>1-3</sup>. It orchestrates cellular responses, e.g. epithelialization, fibroplasia, and angiogenesis, by the regulation of proliferation, differentiation and migration of many cell types during wound healing. Fibroblasts are key players in tissue repair and homeostasis. The ECM synthesizing function of recruited fibroblasts in injured tissue is well-known and leads to collagen and fibronectin (FN) accumulation and its binding to fibrillar fibrin and collagen matrices at wound borders<sup>4-7</sup>.

FN is an important ECM component and plays a crucial role in tissue and wound repair. FN is a multi-domain glycoprotein at a size of 220-250 kDa subunits, which is linked by two c-terminal disulphide bonds to a dimer<sup>8</sup>. FN plays important roles in development<sup>9</sup>, wound repair<sup>10-12</sup> and tumour progression<sup>13,14</sup>. FN is subdivided into 2 types according to its sources, namely plasma and cellular FN<sup>15</sup>. Plasma FN is produced and secreted by hepatocytes into blood plasma, whereas cellular FN is produced by many cell types, including fibroblasts, endothelial cells and chondrocytes. Cellular and plasma FN can be distinguished by the presence of additional polypeptide segments, in particular extra domain A (EDA-FN) and extra domain B (EDB-FN) fragments in the cellular FN. FN contains adhesion promoting sequences, including the most prominent RGD sequence, which can bind specific integrin receptors and stimulates signalling pathways in cell adhesion, migration and differentiation<sup>16,17</sup>. Furthermore, FN is known to directly or indirectly bind multiple soluble factors, including TGF- $\beta$ 1, and presenting it to cell-surface receptors in synergism with integrin mediated adhesion signals<sup>18</sup>.

In the context of wound healing it has been reported that the presence of FN at the wound edge provides the formation of a fibrillar network anchoring cells and molecules for signal transduction as well as induces migration of fibroblasts and epidermal cells toward the wound<sup>19,20</sup>. During the initial phase of wound repair, fibroblasts differentiate into myofibroblasts, characterized by elevated expression of alpha-smooth muscle actin ( $\alpha$ SMA), its incorporation into actin stress fibres and an enhanced ability to contract ECM. Furthermore, myofibroblasts exhibited increased levels of collagen synthesis as well as EDA- and EDB-FN production. TGF- $\beta$ 1 is a well-known

multifunctional cytokine involved in the process of myofibroblast trans-differentiation<sup>21</sup>. Myofibroblasts synthesize tissue matrix proteins like collagen I (Coll I), collagen III and EDA-FN and contribute to wound closure by contracting the ECM. Dysregulation of myofibroblasts may lead to persistence of these matrix producing cells after wound closure resulting in formation of excess fibrous connective tissue in hypertrophic scars and keloids. Furthermore, TGF- $\beta$  may drive pathological ECM deposition in different organs, known as fibrosis. Elucidation of the factors that regulate the trans-differentiation and cellular functions of fibroblasts may thus be useful for identification of therapeutic approaches to accelerate wound repair as well as counteract the fibrosis formation.

As mentioned above, wounds represent a complex microenvironment containing cells, cytokines and various ECM components and their degradation products in a specific composition, mechanics and microstructure<sup>22-26</sup>. In the last years it has become evident, that physiologically relevant *in vitro* cell studies have to use biomimetic 3D scaffolds to appropriately model these ECM parameters and to decipher the contribution of single components. Standard experiments using hard or 2D materials frequently lack predictive power for the *in vivo* cell behaviour<sup>27</sup>. Therefore, 3D synthetic, biohybrid or biopolymer based cell culture scaffolds have been developed, which try to mimic the *in vivo* situation as close as possible<sup>27,28</sup>. In these context collagen I (Coll I) based fibrillar matrices are a well-established tool because (i) collagen is the most abundant ECM protein in mammals, (ii) the fibrillar networks can resemble the *in vivo* 3D microstructure and (iii) present relevant adhesion ligands<sup>29</sup>. However, a controlled functionalization of collagen matrices with other ECM components like FN is frequently hampered by the disturbance of fibril formation by the protein presence. This problem inhibits an independent modulation of collagen network microstructure and an additional functionalization with other ECM components like FN.

In this work, we solve the latter problem by developing a 3D Coll I matrix with adjustable FN functionalization at defined 3D network microstructure. We use this *in vitro* cell culture scaffold to demonstrate the impact of FN in regulating cellular functions i.e. proliferation, migration and differentiation of human dermal fibroblast in the absence and the presence of TGF- $\beta$ 1. Our results allow the dissection of the impact of ECM composition (FN) and growth factor presence (TGF- $\beta$ 1) on fibroblast function in a wound healing context.

## 2 Results and Discussion

The purpose of the first part of this study was to establish topologically and mechanically defined 3D Coll I matrices with an adjustable FN amount. We compared 2 strategies to functionalize Coll I matrices with FN, namely using co-assembly and adsorptive immobilization. Afterwards, FN functionalized Coll I matrices were used to study fibroblasts migration, proliferation and differentiation as an *in vitro* biomimetic wound healing model.

### 2.1 Co-assembly of FN-Coll I matrices

To co-assemble FN with Coll I, mixtures of Coll I and FN were prepared with final concentrations of Coll I of 2 mg/ml and FN of 20, 40, 100 and 200 µg/ml. Coll I fibril formation was initiated at 37 °C and fibrillation kinetic was analysed by turbidity measurements at 405 nm. As shown in Fig. 1A, the time dependence of Coll I fibril formation in absence or presence of FN has a sigmoidal characteristic with typical lag, growth and plateau phases. In the presence of FN, the rate of Coll I fibrillation was higher and a higher final turbidity was observed with increasing FN amount. It is known that an increasing Coll I tropocollagen concentration and/or the presence of other Coll I binding proteins in the fibrillation process, in our case FN, can lead to a faster Coll I fibril formation<sup>30</sup>.

The acceleration of Coll I fibril formation and the increased final turbidity in the presence of FN suggested an alteration in microstructure of Coll I networks. We therefore analysed the Coll I microstructure using confocal laser scanning microscopy (cLSM). FN functionalized 3D Coll I matrices were reconstructed by pipetting the Coll I-FN mixture onto 13 mm PSMA-coated coverslip and fibrillogenesis was performed at 37 °C for 2 h. As shown in Fig. 1B, matrices reconstituted from solutions of 2 mg/ml Coll I concentration showed a homogenous distribution of long Coll I fibrils. In contrast, networks of FN-Coll I mixtures were drastically changed in their microstructure with heterogeneous areas of shorter fibrils. Moreover, reproducibility was much lower in the presence of FN. The microstructure of Coll I networks including pore size, fibril size and connectivity is known to strongly influence the mechanical characteristics of Coll I matrices and the correlated cell behaviour<sup>22,23,25,31-33</sup>. Therefore, co-assembly of Coll I and FN had to be skipped for the preparation of FN functionalized 3D Coll I matrices.

## 2.2 Adsorptive immobilization of FN to reconstituted Coll I matrices

In contrast to co-assembly of Coll I and FN, adsorptive immobilization of FN on Coll I matrices was performed in subsequent steps. Reconstituted fibrillar Coll I matrices (2 mg/ml Coll I, approx. thickness  $200\ \mu\text{m}^{22}$ ) were incubated with FN-TAMRA at different concentrations of 20, 40, 100 and 200  $\mu\text{g/ml}$  at pH 7.4 and 37 °C. FN immobilization kinetic was analysed by enzymatic digestion of Coll I matrices using collagenase after 15, 30, 60, 90, 120 and 180 min of incubation and analysis of the digested solutions by fluorimetry of TAMRA-labelled FN. As shown in Fig. 1C, adsorptive immobilization of FN to Coll I matrices was time-dependent and reached a plateau after 120 min of incubation, which was chosen as incubation time for further experiments. Quantitative analysis of immobilized FN amount revealed 0.05 to 0.45  $\mu\text{g}/\mu\text{g}$  Coll I, enabling adjustable FN amount. The binding stability of FN binding to the matrices could be shown with cell culture medium (DMEM with 10% FCS) for 5 days (Fig. 2A). The analysis of topological and mechanical properties of FN functionalized matrices indicated no alterations in pore size (Fig. 1B and S1) as well as matrix elasticity (Fig. S2). Fibril diameter and length of the used Coll I matrices were recently reported to be 750 nm and 120  $\mu\text{m}$ , respectively<sup>22</sup>. Furthermore, we could show that adsorbed FN was homogeneously distributed in 3D Coll I matrices throughout the whole layer in the vertical direction (Fig. 2B).

Our data show that subsequent adsorptive immobilization of FN to Coll I matrices is a meaningful approach to functionalize topologically and mechanically defined 3D Coll I matrices with adjustable amounts of FN.

## 2.3 Impact of FN and TGF- $\beta$ 1 on fibroblast function in 3D matrices

To demonstrate the advantageous usage of FN functionalized 3D Coll I matrices as a valid biomimetic structure for wound healing processes *in vitro* we studied fibroblast behaviour and differentiation. It has been reported, that cellular parameters like proliferation, migration and differentiation can be mediated by growth factors and are synergistically regulated upon binding to specific ECM ligands<sup>18,34</sup>. TGF- $\beta$ 1 is a promotor of granulation tissue formation *in vivo* and extracellular matrix production *in vitro* and *in vivo* by inducing fibroblasts differentiation into myofibroblasts<sup>21,35</sup>. We aimed on the demonstration of this effect in biomimetic 3D *in vitro* matrices

and the influence of FN presence on this effect since FN is known as an effective modulator of wound healing at early stages *in vivo*<sup>2</sup>.

### 2.3.1 Cell proliferation

Cell viability and number were assessed after 4 days of culture using WST-1 assay, which is based on the cleavage of the tetrazolium salt WST-1 to formazan by cellular mitochondrial dehydrogenases. As shown in Fig. 3, FN content led to a decreased cell number in a dose-dependent manner. In contrast, in the presence of TGF- $\beta$ 1 a reverse effect with a significant increase of cell number was observed in a FN-dose dependent manner.

Integrin-mediated cell adhesion to FN is known to control cell cycle progression via the cyclin-dependent kinase (CDK) signalling pathway<sup>36</sup>. It has been previously reported that TGF- $\beta$ 1 enhances proliferation by induction of basic fibroblast growth factor (FGF-2), resulting in regulation of CDK signalling pathway<sup>37</sup>. Furthermore, FN is known to trigger binding of TGF- $\beta$ 1 via latent TGF-beta binding proteins (LTBP) and fibrillin leading to orchestrated action of integrin and TGF- $\beta$ 1 signalling<sup>18</sup>. While we currently do not have a mechanistic understanding of our findings, our results indicate a multifunctional capacity of FN in reversely regulating proliferation of fibroblasts in dependence on TGF- $\beta$ 1 presence. We suggest this function to be related to the control of TGF- $\beta$ 1 signalling by FN and the overlapping impact of FN and TGF- $\beta$ 1 on proliferation as discussed above. Future studies using well-defined matrices like presented herein are needed to reveal underlying signalling mechanisms.

We have to point out, that there exist contradicting results on FN stimulated fibroblast proliferation in literature.  $\alpha$ 5 $\beta$ 1 integrin-mediated increased fibroblast proliferation was observed in confluent cultures on 2D FN surfaces<sup>38</sup>. Furthermore, it has been reported that FN containing co-assembled 3D Coll I matrices indicated a supportive influence on fibroblast proliferation by FN<sup>39</sup>. However, in both cases the *in vivo* ECM microenvironment is not appropriately mimicked. 2D surface do not recapitulate topology and mechanics of 3D matrices and the co-assembly of Coll I and FN leads to drastic changes in topology and mechanics of pure Coll I matrices as shown above. These changed ECM characteristics are known to strongly influence fibroblast proliferation<sup>24</sup>.

### 2.3.2 3D cell migration

We further analysed the migratory behaviour of fibroblasts in dependence on FN and TGF- $\beta$ 1 presence as fibroblast migration into a regenerating ECM is an important step in wound healing. Migratory behaviour was analysed from microscopy images of DAPI-stained cells by measurement of number and depth of migrated fibroblasts at time point 4 days after seeding on top of the 3D matrices. (Fig. 4A). Cells located  $> 50 \mu\text{m}$  below the Coll I matrix surface were counted as migrated cells. The maximum migration distance was defined as the mean migration distance of 10% of all cells with the highest migration distance. As shown in Fig. 4B and C, an increase in fraction of migrating cells and maximum migration distance were observed with increasing FN amount. In the presence of TGF- $\beta$ 1, cell migration was strongly inhibited and no correlation between cell migration and FN amount was found.

The results demonstrated in agreement with previous studies that FN can activate migration of fibroblast into 3D Coll I matrices, e.g. at wound sites. Integrins, including  $\alpha$ 4 $\beta$ 1,  $\alpha$ v $\beta$ 3 and  $\alpha$ 5 $\beta$ 1, are well-known as FN ligands promoting cell adhesion and migration in a FN dose-dependent manner<sup>40-44</sup>. Furthermore, it has been reported that FN contains a proteolytic fragment in the 120 kDa fibroblastic cell-binding domain that can be released and may promote chemotactic migration<sup>45</sup>. We can exclude other well-known influences on cell migration including network microstructures and mechanics as our new protocol of FN functionalized 3D Coll I matrices leaves these parameters unaffected in dependence on FN amount.

The strong decrease in fibroblast migration by TGF- $\beta$ 1 stimulation is interesting as it indicates a shift in fibroblast phenotype, besides the TGF- $\beta$ 1 and FN-dependent proliferation. TGF- $\beta$ 1 is known to trigger differentiation of fibroblasts into myofibroblast<sup>46,47</sup>, which can influence the proliferative and migratory activities of the cells. A similar decreased migratory activity in pure Coll I matrices under the influence of TGF- $\beta$ 1 is known from earlier studies<sup>4</sup>. Hence, we asked on other indications of myofibroblast differentiation and possible impacts on fibroblast migration in 3D Coll I matrices in the next section.

We finally want to state that although our cells were initially seeded on top of the 3D Coll I matrices, we are confident that we mostly probe a 3D behaviour of cells (proliferation and

differentiation, see below) as most cells are found within the matrix after 4 days. Our stringent method of evaluating migrated cells ignores cells migrating  $< 50 \mu\text{m}$  below the matrix surface. However, Fig. 4B indicates a 3D distribution of all cells. Although there might be some cells still on top of the matrix surface at less motile conditions (TGF- $\beta$ 1 stimulation), we still assume most of the cells within the soft 3D matrix environment of the Coll I layer at these conditions based on the above arguments.

### 2.3.3 Matrix remodelling and cell differentiation

The interaction of fibroblasts and myofibroblasts with the surrounding Coll I matrix involves tensional forces during adhesion and migration as well as reorganization of the matrix by the involved forces and deposited matrix proteins.

Fibroblasts generally have a bipolar or multipolar, and elongated shape. As shown in Fig. 5, FN functionalization of Coll I matrices did not affect fibroblast morphology. Thin actin fibres can be observed in the thin, elongated fibroblasts. In the presence of TGF- $\beta$ 1, the cells exhibited more pronounced stress fibres indicating a differentiation into myofibroblasts. In correlation to these observations we found a higher matrix remodelling by fibroblasts stimulated with TGF- $\beta$ 1, as seen by the highly aggregated FN-modified collagen fibrils next to the cells in Fig. 5 (white arrows), whereas non-stimulated cells tend to remodel Coll I matrices to a much smaller extent. This indication of higher tensional forces of differentiated myofibroblasts was found to be dependent on FN amount with stronger remodelling at higher FN concentration.

The observed changes in tensional state and matrix remodelling activity could be supported by analysis of genes typically associated with myofibroblast differentiation. These genes involve  $\alpha$ SMA for the expression of distinct, highly contractile actin stress fibres and EDA-FN and Coll I for synthesis of new, wound healing associated matrix proteins<sup>46,48-50</sup>. As shown in Fig. 6, TGF- $\beta$ 1 stimulation strongly up-regulated gene expression of  $\alpha$ SMA, EDA-FN and Coll I, independently of FN amount. In non-differentiated fibroblasts (without TGF- $\beta$ 1) a significant down-regulation of these genes was found in presence of FN. The high  $\alpha$ SMA expression in differentiated myofibroblasts is well-known and correlates to our matrix remodelling findings. Furthermore, the high EDA-FN and Coll I gene expression indicate the responsiveness to TGF- $\beta$ 1 leading to a myofibroblast state with

high expression of new matrix proteins.<sup>46</sup> Hence, cellular FN (EDA-FN) production should be up-regulated prospectively leading to a further support of fibroblast differentiation because EDA-FN was recently reported to induce fibroblast differentiation, cell contractility and focal adhesion kinase (FAK) activation via  $\alpha4\beta7$  integrin. In contrast, plasma FN (used to modify Coll I matrices in our study) lacks the EDA fragment and is reported to show less impact on fibroblast differentiation<sup>51</sup>. This is in line with our findings on down-regulation of the discussed genes in the presence of FN without TGF- $\beta$ 1 stimulation. In this context our new matrices could again act as a valuable platform to decipher the differential influences of FN isoforms.

Furthermore, it would be interesting to correlate the amounts of FN in our biomimetic matrices to the *in vivo* situation. Unfortunately, we are not aware of such data of closing wounds. Hence, we can only compare the corresponding cell behaviour of the *in vivo* situation to *in vitro* experiments using our biomimetic matrices of known FN content.

At this stage our data on matrix remodelling activity and fibroblast differentiation can be nicely correlated to the migration data. The high expression of  $\alpha$ SMA and strong stress fibres in differentiated myofibroblasts agree to increased matrix remodelling and decreased motility. In contrast, the decrease in  $\alpha$ SMA expression in non-differentiated fibroblast correlates to an increased migratory activity and negligible matrix remodelling. These findings fit earlier reports on decreased fibroblast migration at differentiating conditions towards myofibroblasts *in vitro*<sup>4</sup> and *in vivo*<sup>52</sup>. This correlation indicates (i) the role of FN in supporting a migratory, less differentiated fibroblast phenotype when TGF- $\beta$ 1 is absent and (ii) the importance of TGF- $\beta$ 1 to support myofibroblasts differentiation in a FN independent manner in this biomimetic system. It shows that we can nicely model important subsequent steps of *in vivo* wound healing, namely (i) fibroblast migration in a permissive FN rich peri-wound and (ii) the subsequent TGF- $\beta$ 1 controlled myofibroblast differentiation within the wound site.

It has to be pointed out that the distinction of the dose-dependent impact of FN functionalization on fibroblast proliferation and differentiation is based on the ability to modify 3D Coll I matrix with FN without the disturbance of its topological and mechanical properties. Otherwise well-known influences of matrix microstructure and mechanics on fibroblast behaviour could have misled our experiments.

Fibroblast morphology and stress fibre formation strongly depends on mechanical parameters of Coll I matrices. No stress fibres and few focal adhesion were reported in a floating Coll I matrix<sup>53</sup>, which relates to a low tensional state of the fibroblast. In a high tension state, fibroblasts exhibit strong formation of stress fibres and focal adhesions<sup>54</sup>. Our topological and mechanically defined matrices allow us to rule out such influences on cell behaviour.

### 3 Conclusions

We demonstrated the adsorptive immobilization of FN in 3D Coll I matrices as an advantageous approach to provide a defined microstructure and mechanics of biomimetic ECM independent of functionalization with adjustable FN amount. Fibroblast behaviour at differentiating and non-differentiating conditions towards myofibroblasts indicated an overlapping action of FN functionalization and TGF- $\beta$ 1 presence for proliferative activity underpinning the multifunctional role of FN as adhesion ligand, cell cycle regulator and growth factor presenter. Furthermore, migratory activity was specifically regulated at these conditions.

Our studies in defined biomimetic 3D matrices can distinguish the impact of matrix mechanics, adhesion ligands and growth factor presence, in contrast to contradicting previous reports<sup>39,55,56</sup>. They are able to mimic several features of the *in vivo* behaviour of fibroblasts in wound healing. Fibroblast transmigrate from the peri-wound, the close wound surrounding, with its high amount of FN into the fibrin and FN rich wound matrix<sup>41</sup>. At the wound site, fibroblasts differentiate by TGF- $\beta$ 1 expressed by macrophages and other cells towards myofibroblasts. In this situation they proliferate and become activated for matrix remodelling, while decreasing migratory activity. All these processes can be captured within our model suggesting these new 3D biomimetic matrices for other *in vitro* cell studies. Further application of these matrices will enable the dissection of the impact of important cues of the cellular microenvironments including ECM properties and soluble factor action in studies on wound healing, tumour progression as well as stem cell homeostasis.

## 4 Experimental section

### 4.1 Isolation and labelling of human plasma FN

Fresh human plasma was provided from Blutbank, Universitätsklinikum Leipzig, after informed consent. FN was isolated by affinity chromatography using gelatine agarose (Sigma-Aldrich, Germany) and heparin sepharose 6 fast flow columns, (GE Healthcare, Germany)<sup>57</sup>. Purified FN was labelled with 5-(and-6)-Carboxytetramethylrhodamine succinimidyl ester (TAMRA; Invitrogen, Carlsbad, CA)<sup>58</sup>.

#### **4.2 Kinetic study of Coll I fibrillogenesis**

Type I rat tail collagen (Corning, Germany) was mixed with prepared FN solution and dissolved in 0.43 M phosphate buffer at pH 7.5 to achieved 2 mg/ml Coll I concentration and 20, 40, 100 and 200 µg/ml FN concentration. Coll I preparation was performed on ice (4 °C) to prevent Coll I fibrillogenesis. For fibrillogenesis studies, 100 µl of prepared Coll I solutions was transferred into pre-chilled (4 °C) 96-well microplates. Microplates were loaded into a pre-warmed (37 °C) plate reader (Tecan Infinite F200Pro, Tecan, Grödig, Austria) and the turbidity at 405 nm was measured at 1 min intervals for 60 min. Measurements were performed at least in triplicates.

#### **4.3 Reconstitution of 3D Coll I matrices**

Coll I matrices were reconstituted on 13 mm glass coverslip coated with 0.14% w/w poly(styrene-alt-maleic anhydride) (PSMA; MW 30000 g/mol; Sigma-Aldrich) according to previous reports<sup>59</sup>. Coll I mixtures or pure Coll I solutions were prepared as stated above (4.2). Subsequently, the mixtures were transferred onto glass coverslip<sup>22</sup>. Coll I fibrillogenesis was initiated for 90 min at 37 °C, 5% CO<sub>2</sub>. Fibrillated Coll I matrices were rinsed 3 times with phosphate buffered saline (PBS, Biochrom, Berlin, Germany) prior to analysis, functionalization or cell experiments. Fibrillated Coll I amount was analysed using Bradford assay<sup>23</sup>.

#### **4.4 Adsorptive immobilization of FN**

For functionalization of 3D Coll I matrices with adsorptive FN, reconstituted 3D matrices were incubated with FN solution in PBS at 20, 40, 100 and 200 µg/ml concentration (FN labelled or unlabelled with TAMRA) for 2 h at 37 °C, 5% CO<sub>2</sub> and 95 % humidity. FN immobilized matrices were rinsed 3 times with PBS prior to use.

#### 4.5 Analysis of immobilized FN amount and Coll I matrix topology and mechanics

Coll I matrices with and without FN functionalization were enzymatically digested using 2 mg/ml collagenase (250 U/ml; Biochrom AG, Berlin, Germany) with shaking at 1 minute intervals for 15 min at 37 °C. The amount of immobilized FN was determined by fluorimetry (absorption: 535 nm, emission: 590 nm) using a plate reader (Tecan Infinite F200Pro). Measurements were performed in triplicates. For studies on adsorption kinetic, FN amount immobilized in the matrices was quantified after 0, 15, 30, 60, 90, 120 and 180 min of incubation.

Homogeneity of FN distribution throughout the Coll I matrix was analysed using cLSM (LSM 700, Zeiss, Jena, Germany) stack images of FN-TAMRA fluorescent signal. The images were acquired using 40× /NA 1.3 oil immersion objective and 1024 × 1024 pixels in resolution and a vertical stack size of 10 images (equivalent to 50 µm). The voxel size of the acquired images was 0.13 × 0.13 × 5 µm (x × y × z). The FN-TAMRA fluorescent signal in z-direction was normalized to a reference from FN-TAMRA solution of 473 µg/ml.

Network topology and mechanics of FN functionalized Coll I networks was analysed as previously reported<sup>22,23</sup>.

#### 4.6 Cell culture

Primary human dermal fibroblasts from foreskin were isolated as previously described<sup>60</sup> after informed consent and were expanded up to 4<sup>th</sup> passage. Fibroblasts were seeded onto prepared 3D Coll I matrices and cultured with Dulbecco's modified Eagle's medium (DMEM; Biochrom AG, Berlin, Germany) supplemented with 10 vol.% fetal calf serum (FCS; Biochrom) and 1 vol.% ZellShield (antibiotic) (Biochrom) at 37 °C, 5% CO<sub>2</sub> and 95% humidity, either untreated or treated with 5 ng/ml TGF-β1 (Peprotech, Hamburg, Germany) after 1 day of cultivation.

#### 4.7 Analysis of cell proliferation

Cell proliferation was determined after 4 days by means of commercial WST-1 assay (Roche, Germany). Cells were rinsed 3x with Hanks' balanced salt solution (HBSS; Biochrom) with Ca<sup>2+</sup> and Mg<sup>2+</sup> and were subsequently incubated for 2 h with 500 µl WST-1 solution (1:10 dilution with cell

culture medium) at cell culture condition. Supernatants were collected and 100  $\mu$ l of each supernatant were transferred to 96-well plates. Absorbance was measured at 450 nm with a multi-well plate reader.

#### **4.8 Analysis of cell migration and morphology**

Cell migration was determined by number and depth of migrated cells after 4 days of culture. For analysis, cells were fixed in 4% paraformaldehyde (Roth, Karlsruhe, Germany) and permeabilized with 0.1% Triton X100 (Roth, Germany). Nuclei and F-actin of cells were stained with DAPI (Invitrogen, Germany) and Alexa Fluor 488 Phalloidin (Invitrogen, Germany), respectively. Cells were imaged with 40 $\times$ /NA 1.3 oil immersion objective using cLSM (LSM 700). Experiments were performed in three independent experiments.

Cell migration was quantified by analysing DAPI signal from individual cell nuclei. Stacked images were gathered using an epifluorescence microscope with scanning stage (AxioObserver.Z1, Zeiss) using a 10 $\times$  objective (1388 $\times$ 1040 pixels in resolution with 5  $\mu$ m z-distance). For each cell migration experiment, at least 200 cells at 3 positions from 3 independent experiments were analysed per experimental condition. The z-position of cell nuclei as a function of migration distance below Coll I matrix surface was examined using a custom-written Matlab (Matlab R2014a; MathWorks Inc, USA) script. Cells located > 50  $\mu$ m below the Coll I matrix surface were counted as migrated cells. The maximum migration distance was defined as the mean migration distance of 10% of all cells with the highest migration distance.

#### **4.9 Expression analysis of tissue remodelling genes**

3D matrices were provided in 24-well plates and incubated with  $1 \times 10^4$  fibroblasts per well for 96 h at indicated cell culture conditions. For quantitative real-time polymerase chain reaction (RT-qPCR) analysis, Coll I matrices were functionalized with unlabelled FN. RNA isolation and qRT-PCR procedures were performed as previously described<sup>61</sup>. Total RNA was isolated using Qiagen RNeasy Micro Kit (Qiagen, Hilden, Germany) and RNA amount was determined by spectrophotometry (ND-1000, Nano Drop Technologies, Wilmington, DE). The synthesis of cDNA was performed as previously described<sup>62</sup> using 1  $\mu$ g total RNA. RT-qPCR was performed with a Rotor-Gene Q cycler (Qiagen) using GoTaq<sup>®</sup> qPCR Master Mix (Promega Corporation, Madison, WI). The primers for

aSMA, FN-EDA, Coll I and rps26 (reference gene) genes were synthesized by Metabion International AG (Martinsried, Germany) (Tab. S1). The PCR procedure was set as follow: denaturation for 5 min at 95 °C; 28–40 amplifications of denaturation (10 s at 92 °C), annealing under primer-specific conditions (20 s) and target gene-specific extension (30 s at 61 °C). Fluorescence measurement was conducted for 20 s at 80–82 °C depending on the melting temperature of the amplified DNA. The specificity of the PCR products was confirmed by melting curve analysis at the end of each run. Genes were normalized to the unregulated reference gene rps26<sup>63</sup>. Results are expressed as fold induction with respect to 3D matrices without FN and TGF-β1 treatment.

#### 4.10 Statistical analysis

Experiments were performed at least in triplicate, if not otherwise stated. Error bars indicate standard deviation (SD). Levels of statistical significance were determined using an unpaired t-test using OriginPro 8 (OriginLab Corp., USA). Significance level was set at  $p \leq 0.05$ .

#### Acknowledgements

The authors acknowledge the support of grants from ESF 'European Social Funds' and Free State of Saxony (SAB, grant: 100147954), from Deutsche Forschungsgemeinschaft (DFG, grant: SFB-TR67/B10,B4 and INST 268/293-1 FUGG) and from Human Frontier Science Program Organisation (HFSPO RGP0051/2011). We thank Tina Koenig, Ilja Iwlew and Annett Majok for assistance in FN isolation, preparation of PSMA-coated coverslips and qPCR, respectively. Technical discussions with Michael Ansorge, Katja Franke and Liv Kalbitzer are gratefully acknowledged.

**Figure Captions**

**Fig. 1:** FN functionalization of Coll I matrices using co-assembly and adsorptive immobilization strategies. (A) Kinetic study of Coll I fibrillogenesis (concentration 2 mg/ml Coll I) in the absence and presence of FN at concentration of 20, 40, 100 and 200  $\mu\text{g/ml}$ . Fibrillogenesis kinetic was measured at 405 nm for 60 min (at 1 min intervals) at 37 °C. Results are representative from 3 independent experiments. (B) Representative images of Coll I matrix microstructures either non-functionalized, with FN co-assembly or adsorptive immobilization of FN. (C) Adsorptive immobilization kinetic of FN at concentrations of 20, 40, 100 and 200  $\mu\text{g/ml}$  in reconstituted Coll I matrices (2 mg/ml) (n=3; mean $\pm$ SD).

**Fig. 2:** Quantitative analysis and distribution of FN with adsorptive immobilization in Coll I matrices. (A) Stability and amount of adsorptively immobilized TAMRA-labelled FN in Coll I matrices was determined during incubation in DMEM cell culture medium with 10% FCS supplement at 1 day and 5 days of incubation using by fluorimetry. (n=3; mean $\pm$ SD). (B) Homogeneity of FN distribution throughout Coll I layer thickness. Fluorescent intensity of labelled FN from cLSM images of adsorptive functionalized 3D Coll I matrices was normalized to labelled FN solution at concentration of 478  $\mu\text{g/ml}$ . Data are representative of three independent experiments.

**Fig. 3:** Proliferation of fibroblasts in 3D matrices in the presence of FN with and without stimulation with 5 ng/ml TGF- $\beta$ 1. Cell proliferation was analysed using commercial WST-1 assay (n=3; mean $\pm$ SD; \*,#,§: significant difference  $p \leq 0.05$ ; #: significantly different compared to samples without FN and without TGF- $\beta$ 1; §: significantly different compared to samples without FN and with TGF- $\beta$ 1).

**Fig. 4:** Migration of fibroblasts into 3D Coll I matrices is dependent of FN amount and TGF- $\beta$ 1 stimulation. (A) and (B) show the principle of migration analysis for the example of 20  $\mu\text{g/ml}$  FN

without TGF- $\beta$ 1. Cells located  $>50 \mu\text{m}$  below the Coll I matrix surface were counted as migrated cells. The maximum migration distance was defined as the mean migration distance of 10% of all cells with the highest migration distance. (C) Fraction of cells migrated into Coll I matrices and (D) maximum migration distance. (n=3 with 3 positions for each Coll I matrices; mean $\pm$ 90% confidential interval; \*,#: significant difference  $p \leq 0.05$ ; #: significantly different compared to samples without FN and without TGF- $\beta$ 1).

**Fig. 5:** Matrix microstructure and fibroblast morphology. Fibroblasts were cultured for 4 days in the presence of FN with and without stimulation with 5 ng/ml TGF- $\beta$ 1. cLSM images show Coll I fibrils (white), FN (red), nuclei (blue), actin filaments (green). White arrows indicate strong matrix remodelling by differentiated myofibroblasts. Representative images out of 3 independent assays are shown. (Scale bar: 50  $\mu\text{m}$ ).

**Fig. 6:** Gene expression analysis of fibroblasts grown in FN-loaded Coll I matrices using RT-qPCR. Fibroblasts were cultivated in the presence of FN with and without stimulation with TGF- $\beta$ 1 (5ng/ml) and were lysed after 4 days of cultivation. RT-qPCR experiment were preformed to analyse gene regulation of (A) alpha-smooth muscle actin, (B) alpha I chain of Coll I and (C) FN with EDA fragment (n=3; mean $\pm$ SD; \*,#: significant difference  $p \leq 0.05$ ; #: significantly different compared to samples without FN and without TGF- $\beta$ 1).

## References

- 1 G. S. Schultz and A. Wsocki, *Wound Repair Regen.*, 2009, 17, 153–162.
- 2 P. Olczyk, Ł. Mencner and K. Komosinska-Vassev, *Biomed Res. Int.*, 2014, 2014.
- 3 M. G. Tonnesen, X. Feng and R. A. F. Clark, in *Journal of Investigative Dermatology Symposium Proceedings*, 2000, vol. 5, pp. 40–46.
- 4 F. Grinnell, *Trends Cell Biol.*, 2003, 13, 264–269.
- 5 S. H. Phan, *Proc. Am. Thorac. Soc.*, 2008, 5, 334–337.

- 6 S. E. Herrick, P. Sloan, M. McGurk, L. Freak, C. N. McCollum and M. W. Ferguson, *Am. J. Pathol.*, 1992, 141, 1085–1095.
- 7 J. A. Ortiz-Rey, J. M. Suárez-Pearanda, E. a. Da Silva, J. I. Muoz, P. San Miguel-Fraile, a. De la Fuente-Buceta and L. Concheiro-Carro, *Forensic Sci. Int.*, 2002, 126, 118–122.
- 8 R. Pankov and K. M. Yamada, *J. Cell Sci.*, 2002, 115, 3861–3863.
- 9 A. Mittal, M. Pulina, S. Y. Hou and S. Astrof, *Mech Dev*, 2010, 127, 472–484.
- 10 F. Grinnell, R. E. Billingham and L. Burgess, *J. Invest. Dermatol.*, 1981, 76, 181–189.
- 11 D. C. Roy, N. A. Mooney, C. H. Raeman, D. Dalecki and D. C. Hocking, *Tissue Eng Part A*, 2013, 19, 2517–2526.
- 12 L. V. Valenick, H. C. Hsia and J. E. Schwarzbauer, *Exp. Cell Res.*, 2005, 309, 48–55.
- 13 N. Balanis, M. K. K. Wendt, B. J. J. Schiemann, Z. Wang, W. P. P. Schiemann and C. R. R. Carlin, *J. Biol. Chem.*, 2013, 288, 17954–67.
- 14 K. Wang, R. C. C. Andresen Eguiluz, F. Wu, B. R. R. Seo, C. Fischbach and D. Gourdon, *Biomaterials*, 2015, 54, 63–71.
- 15 W. S. To and K. S. Midwood, *Fibrogenes. Tissue Repair*, 2011, 4, 21.
- 16 R. O. O. Hynes, *Cell*, 2002, 110, 673–687.
- 17 E. H. J. H. J. Danen and A. Sonnenberg, *J. Pathol.*, 2003, 201, 632–641.
- 18 R. O. Hynes, *Science*, 2009, 326, 1216–1219.
- 19 A. Takashima, R. E. Billingham and F. Grinnell, *J. Invest. Dermatol.*, 1986, 86, 585–590.
- 20 P. Knox, S. Crooks and C. S. Rimmer, *J. Cell Biol.*, 1986, 102, 2318–2323.
- 21 A. Leask and D. J. Abraham, *FASEB J.*, 2004, 18, 816–827.
- 22 J. Sapudom, S. Rubner, S. Martin, T. Kurth, S. Riedel, C. T. Mierke and T. Pompe, *Biomaterials*, 2015, 52, 367–375.
- 23 K. Franke, J. Sapudom, L. Kalbitzer, U. Anderegg and T. Pompe, *Acta Biomater.*, 2014, 10, 2693–2702.
- 24 E. Hadjipanayi, V. Mudera and R. A. Brown, *J. Tissue Eng. Regen. Med.*, 2009, 3, 77–84.
- 25 C. Branco da Cunha, D. D. Klumpers, W. A. Li, S. T. Koshy, J. C. Weaver, O. Chaudhuri, P. L. Granja and D. J. Mooney, *Biomaterials*, 2014, 35, 8927–8936.

- 26 S. Meran, D. Thomas, P. Stephens, J. Martin, T. Bowen, A. Phillips and R. Steadman, *J. Biol. Chem.*, 2007, 282, 25687–25697.
- 27 B. M. Baker and C. S. Chen, *J. Cell Sci.*, 2012, 125, 3015–3024.
- 28 M. E. Smithmyer, L. A. Sawicki and A. M. Kloxin, *Biomater Sci*, 2014, 2, 634–650.
- 29 M. D. Shoulders and R. T. Raines, *Annu. Rev. Biochem.*, 2009, 78, 929–958.
- 30 E. Kadler and J. Prockops, 1987, 260, 15696–15701.
- 31 N. A. Kurniawan, S. Enemark and R. Rajagopalan, *J Chem Phys*, 2012, 136, 65101.
- 32 K. Wolf, M. Te Lindert, M. Krause, S. Alexander, J. Te Riet, A. L. Willis, R. M. Hoffman, C. G. Figdor, S. J. Weiss and P. Friedl, *J Cell Biol*, 2013, 201, 1069–1084.
- 33 J. T. Erler and V. M. Weaver, *Clin. Exp. Metastasis*, 2009, 26, 35–49.
- 34 R. A. F. Clark, G. A. McCoy, J. M. Folkvord and J. M. McPherson, *J. Cell. Physiol.*, 1997, 170, 69–80.
- 35 A. Desmoulière, A. Geinoz, F. Gabbiani and G. Gabbiani, *J. Cell Biol.*, 1993, 122, 103–111.
- 36 M. A. Schwartz and R. K. Assoian, *J. Cell Sci.*, 2001, 114, 2553–2560.
- 37 F. Strutz, M. Zeisberg, A. Renziehausen, B. Raschke, V. Becker, C. van Kooten and G. Müller, *Kidney Int.*, 2001, 59, 579–592.
- 38 M. Tanaka, T. Abe and Y. Hara, *J. Cell. Physiol.*, 2009, 219, 194–201.
- 39 C. A. Sevilla, D. Dalecki and D. C. Hocking, *Tissue Eng. Part A*, 2010, 16, 3805–3819.
- 40 K. M. Yamada and R. a F. Clark, *Mol. Cell. Biol. wound repair*, 1996, 51–93.
- 41 R. A. F. Clark, F. Lin, D. Greiling, J. An and J. R. Couchman, *J. Invest. Dermatol.*, 2004, 122, 266–277.
- 42 C. Wu, A. J. Fields, B. A. Kapteijn and J. a McDonald, *J. Cell Sci.*, 1995, 108 ( Pt 2, 821–829.
- 43 M. A. Schwartz, M. D. Schaller and M. H. Ginsberg, *Annu. Rev. Cell Dev. Biol.*, 1995, 11, 549–599.
- 44 F. G. Giancotti and E. Ruoslahti, *Science*, 1999, 285, 1028–1032.
- 45 R. A. F. Clark, N. E. Wikner, D. E. Doherty and D. a. Norris, *J. Biol. Chem.*, 1988, 263, 12115–12123.
- 46 J. J. Tomasek, G. Gabbiani, B. Hinz, C. Chaponnier and R. A. Brown, *Nat. Rev. Mol. Cell Biol.*, 2002, 3, 349–363.

- 47 A. Desmoulière, C. Guyot and G. Gabbiani, *Int. J. Dev. Biol.*, 2004, 48, 509–517.
- 48 J. J. Santiago, A. L. Dangerfield, S. G. Rattan, K. L. Bathe, R. H. Cunnington, J. E. Raizman, K. M. Bedosky, D. H. Freed, E. Kardami and I. M. C. Dixon, *Dev. Dyn.*, 2010, 239, 1573–1584.
- 49 B. Hinz, S. H. Phan, V. J. Thannickal, A. Galli, M.-L. Bochaton-Piallat and G. Gabbiani, *Am. J. Pathol.*, 2007, 170, 1807–1816.
- 50 L. F. Castella, L. Buscemi, C. Godbout, J.-J. Meister and B. Hinz, *J. Cell Sci.*, 2010, 123, 1751–1760.
- 51 M. Kohan, A. F. Muro, E. S. White and N. Berkman, *FASEB J.*, 2010, 24, 4503–4512.
- 52 B. Hinz, *J. Invest. Dermatol.*, 2007, 127, 526–537.
- 53 S. Rhee, *Exp. Mol. Med.*, 2009, 41, 858–865.
- 54 W. M. Petroll and L. Ma, *Cell Motil. Cytoskeleton*, 2003, 55, 254–264.
- 55 M. Jarman-Smith, T. Bodamyali, C. Stevens, J. A. Howell, M. Horrocks and J. B. Chaudhuri, *Biochem. Eng. J.*, 2004, 20, 217–222.
- 56 C. Helary, L. Ovtracht, B. Coulomb, G. Godeau and M. M. Giraud-Guille, *Biomaterials*, 2006, 27, 4443–4452.
- 57 T. F. Busby, W. S. Argraves, S. A. Brew, I. Pechik, G. L. Gilliland and K. C. Ingham, *J. Biol. Chem.*, 1995, 270, 18558–18562.
- 58 L. Renner, T. Pompe, K. Salchert and C. Werner, *Langmuir*, 2004, 20, 2928–2933.
- 59 T. Pompe, S. Zschoche, N. Herold, K. Salchert, M. F. Gouzy, C. Sperling and C. Werner, *Biomacromolecules*, 2003, 4, 1072–1079.
- 60 A. Saalbach, C. Klein, C. Schirmer, W. Briest, U. Anderegg and J. C. Simon, *J Invest Dermatol*, 2010, 130, 444–454.
- 61 A. van der Smissen, S. Samsonov, V. Hintze, D. Scharnweber, S. Moeller, M. Schnabelrauch, M. T. Pisabarro and U. Anderegg, *Acta Biomater*, 2013, 9, 7775–7786.
- 62 M. Abe, J. G. Harpel, C. N. Metz, I. Nunes, D. J. Loskutoff and D. B. Rifkin, *Anal Biochem*, 1994, 216, 276–284.
- 63 S. Vincent, L. Marty and P. Fort, *Nucleic Acids Res.*, 1993, 21, 1498.

**Table of Contents Entry**

TGF- $\beta$ 1 dependent fibroblast behaviour is mimicked by topologically and mechanically defined collagen matrices with fibronectin functionalization in a wound healing context.

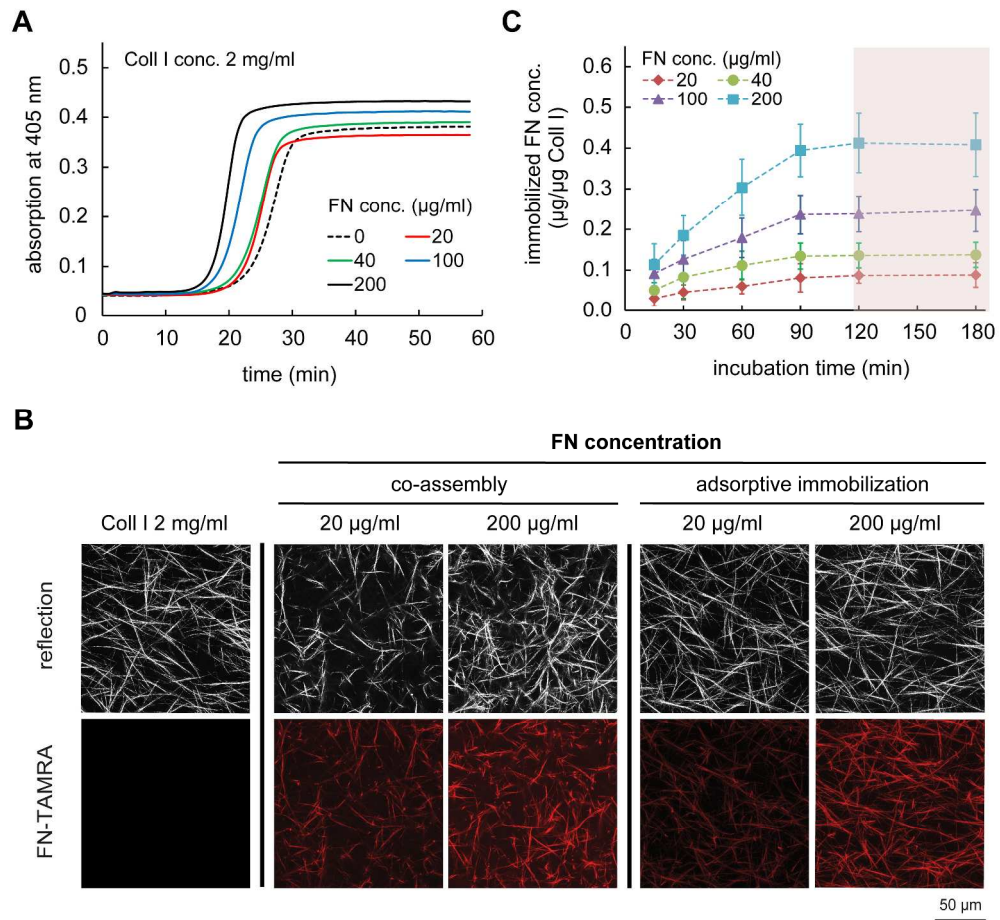
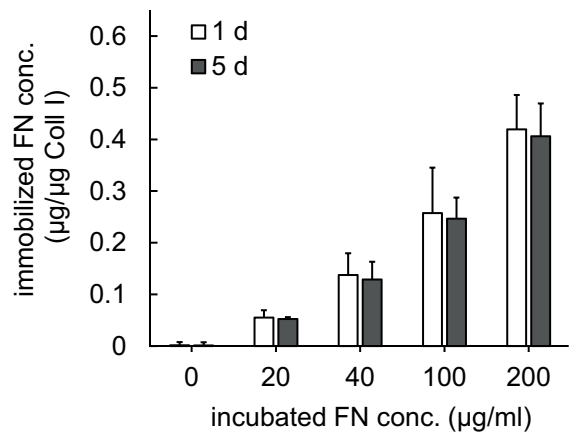
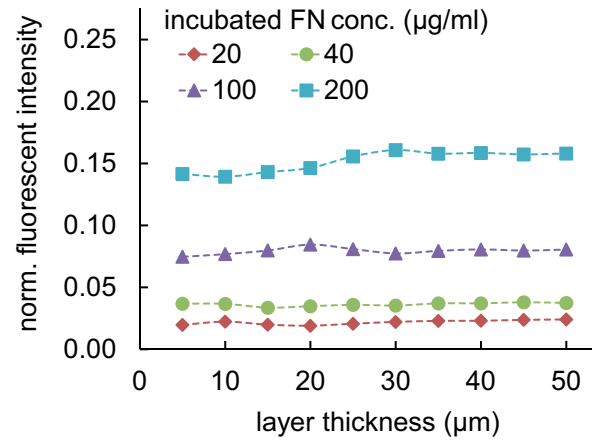


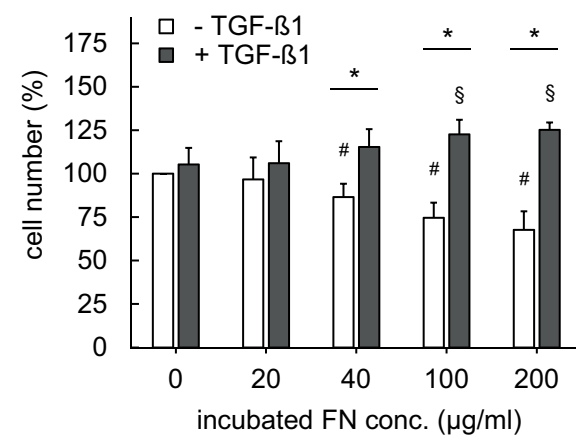
Figure1  
159x148mm (600 x 600 DPI)

**A**



**B**





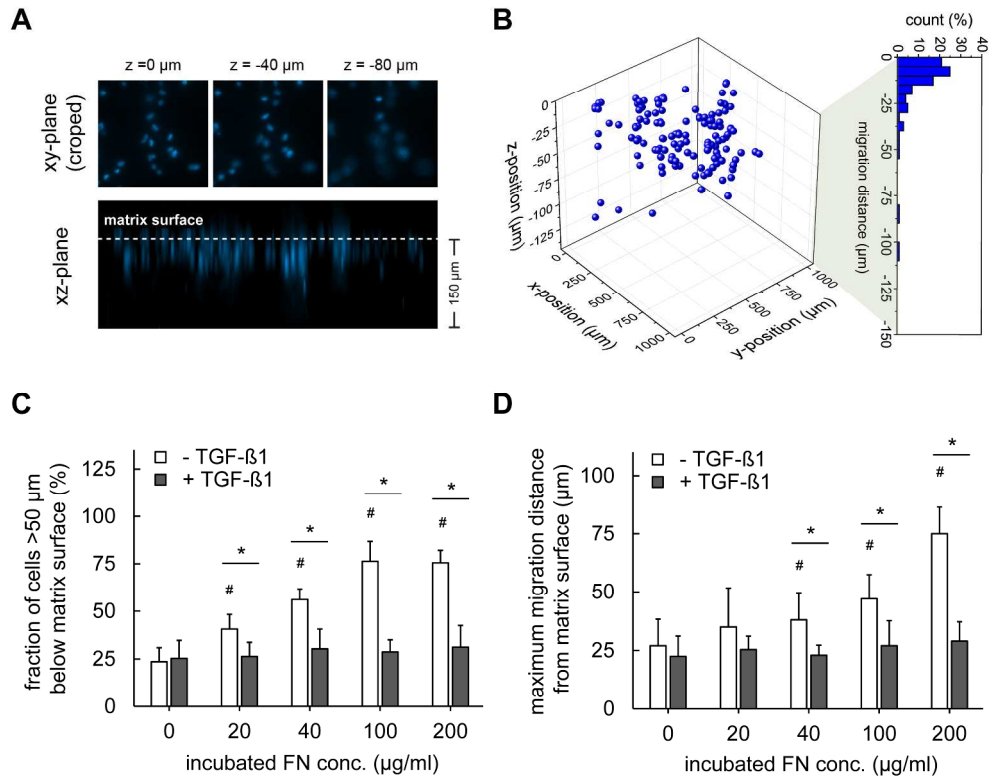


Figure4  
136x109mm (600 x 600 DPI)

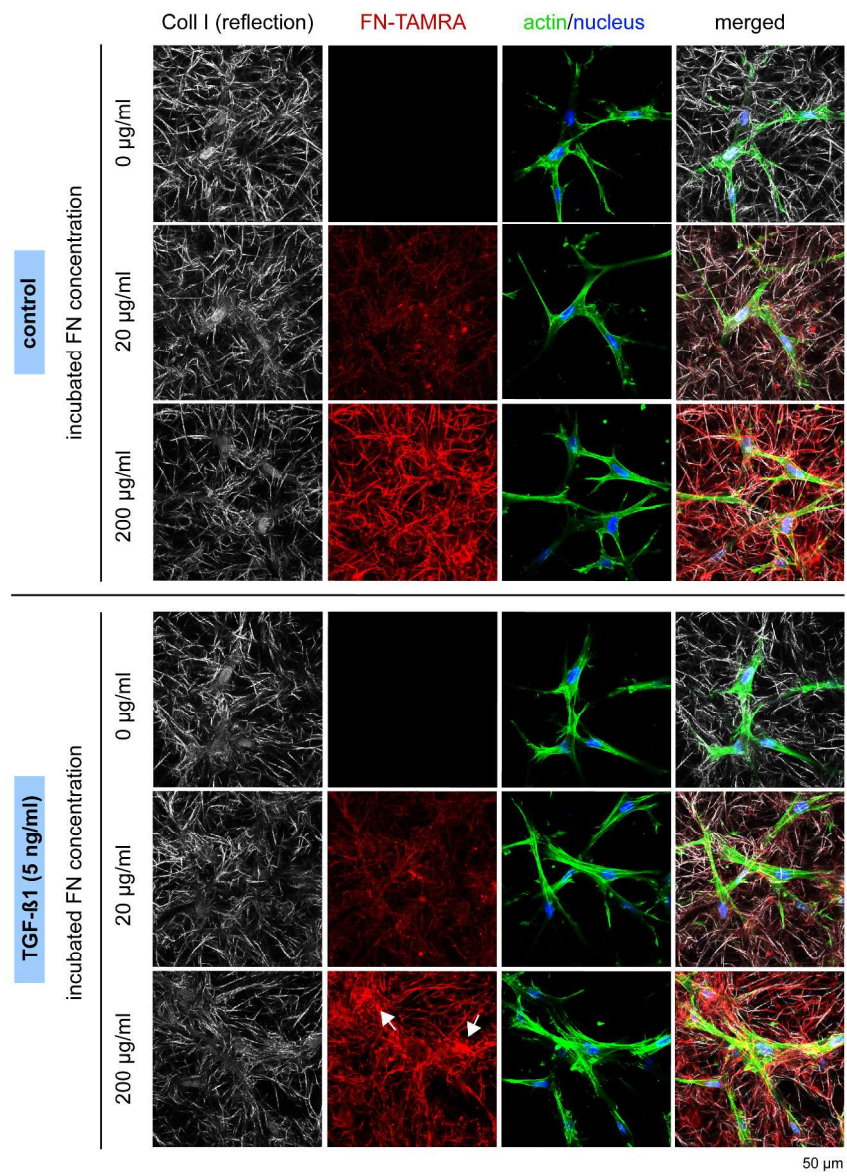
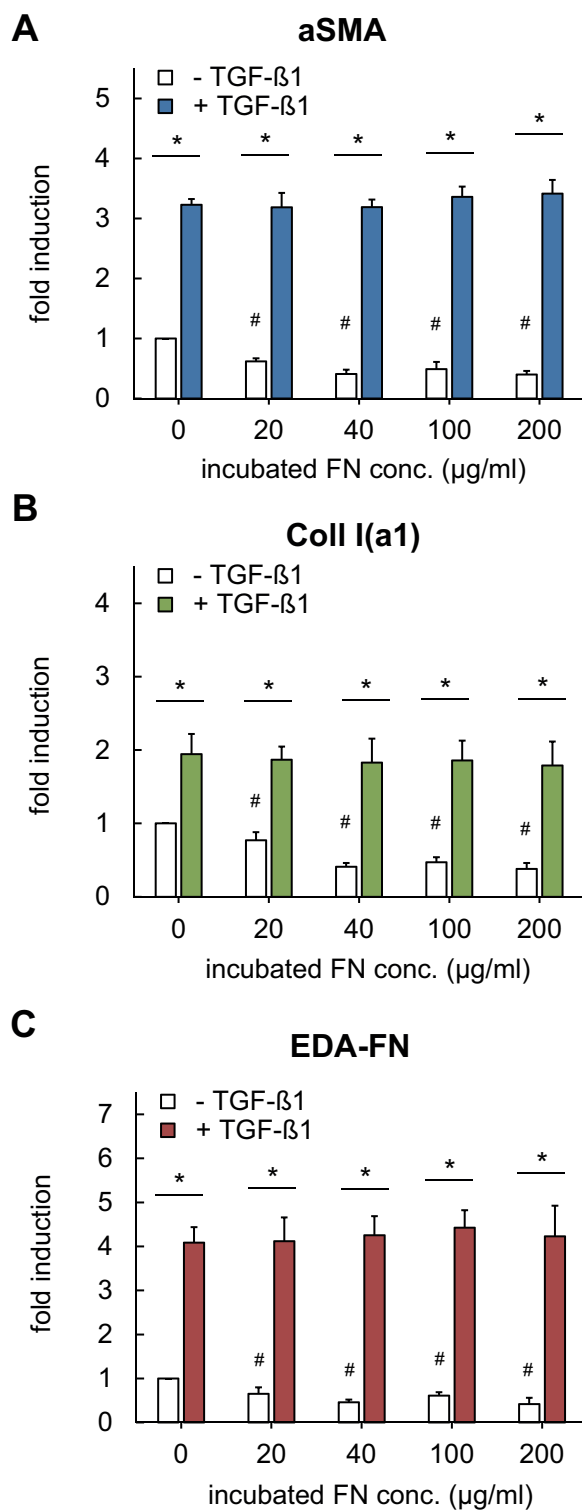
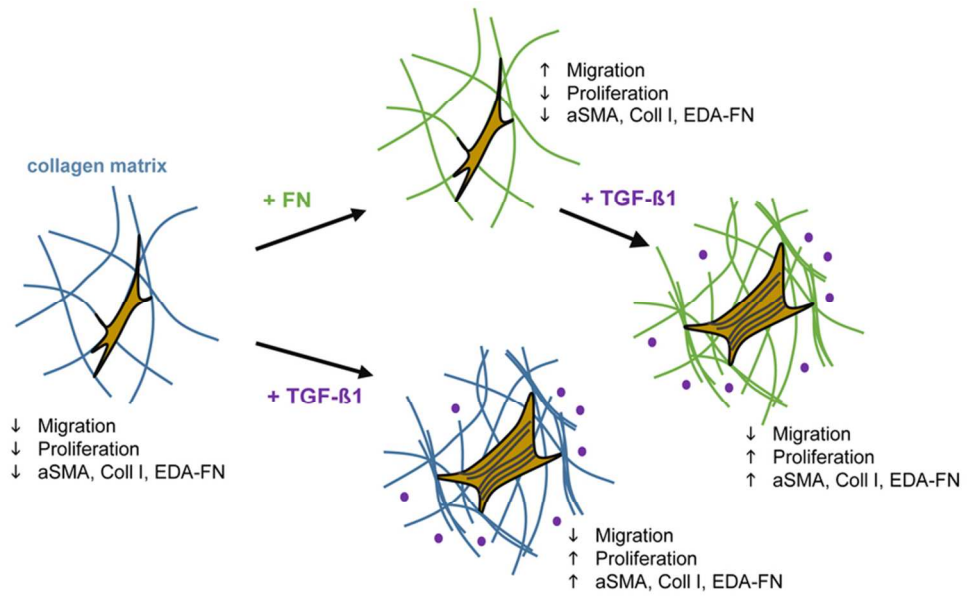


Figure5  
202x277mm (600 x 600 DPI)





Graphical Abstract  
40x24mm (600 x 600 DPI)